Railway transition zones

evaluation of existing transition structures and a newly proposed transition structure

Jain, A.; Metrikine, A.V.; Steenbergen, M.J.M.M.; van Dalen, K.N.

DOI
10.1080/23248378.2023.2272668

Publication date
2023

Document Version
Final published version

Published in
International Journal of Rail Transportation

International Journal of Rail Transportation

ISSN: (Print) (Online) Journal homepage: https://www.tandfonline.com/loi/tjrt20

Railway transition zones: evaluation of existing transition structures and a newly proposed transition structure

A. Jain, A.V. Metrikine, M.J.M.M. Steenbergen & K.N. van Dalen

To cite this article: A. Jain, A.V. Metrikine, M.J.M.M. Steenbergen & K.N. van Dalen (26 Oct 2023): Railway transition zones: evaluation of existing transition structures and a newly proposed transition structure, International Journal of Rail Transportation, DOI: 10.1080/23248378.2023.2272668

To link to this article: https://doi.org/10.1080/23248378.2023.2272668

INTERNATIONAL JOURNAL OF RAIL TRANSPORTATION
https://doi.org/10.1080/23248378.2023.2272668

Taylor & Francis
Taylor & Francis Group

Railway transition zones: evaluation of existing transition structures and a newly proposed transition structure

A. Jain, A.V. Metrikine, M.J.M.M. Steenbergen and K.N. van Dalen

Faculty of Civil Engineering and Geosciences (CEG), Department of Engineering Structures, TU Delft, Delft, The Netherlands

ABSTRACT

This comprehensive study addresses the persistent issue of railway transition zone degradation, evaluating the efficacy of the most commonly used mitigation measures and proposing a novel Safe Hull-Inspired Energy Limiting Design (SHIELD) of a transition structure. Firstly, this work assesses the traditional transition structures, including horizontal and inclined approach slabs and transition wedges, using commonly studied responses (kinematic response and stress) and a recently proposed criterion based on total strain energy minimization. The second part of the paper evaluates the newly introduced transition structuress (SHIELD) using the same criterion as used for the evaluation of the traditional transition structures. A detailed investigation of existing and a new design using a 2-dimensional finite element model shows SHIELD's effectiveness in managing energy flow at transition zones and provides reasoning behind the ineffectiveness of the other commonly used transition structures. The study demonstrates the robustness and comprehensiveness of the recently developed energy-based criterion and its applicability to different types of transition zones. Moreover, it highlights the potential of SHIELD as a solution to address the complexities associated with the design of railway transition zones.

ARTICLE HISTORY
Received 10 July 2023
Revised 12 October 2023
Accepted 16 October 2023

KEYWORDS
Railway transition zones; horizontal approach slab; inclined approach slab; transition wedge; new transition structure; design evaluation

1. Introduction

The degradation of railway transition zones [1–6] has been a persistent problem for several years and despite the various mitigation measures [1,2,7–13] that have been adopted, a robust design solution has yet to be found. Approach slabs and transition wedges have been commonly used in railway transition zones to reduce the problem, but their effectiveness has been questionable. These measures have in some cases proved to be either inefficient or even counterproductive [2]. Therefore, it is necessary to evaluate the existing mitigation measures with a valid design criterion and understand the reasons behind their ineffectiveness. Factors such as the soil type [14,15], the geometric parameters of the transition structure, the depth of the track-bed layers (ballast, embankment) [16,17], and the speed of the passing trains also play a major role in determining the performance of these transition structures. However, the performance and sensitivity of the design solutions to the factors mentioned above can be controlled by engineers by carefully evaluating the transition structure using a reliable design criterion. In this work, keeping the abovementioned

CONTACT A. Jain A.jain-1@tudelft.nl Faculty of Civil Engineering and Geosciences (CEG), Department of Engineering Structures, TU Delft, Stevinweg 1, Delft 2628 CN, The Netherlands

factors constant, different types of transition structures will be evaluated using the criterion discussed below. The purpose of this paper is twofold. Firstly, it aims to evaluate existing design solutions for railway transition zones using a robust design criterion and provide reasoning behind their inefficiency. Secondly, the paper proposes a novel, Safe Hull-Inspired Energy Limiting Design (SHIELD) of railway transition zones based on the study presented by the authors in [18] that highlights the importance of eliminating the obstruction of energy flow as much as possible in transition zones and by guiding it away from the trackbed layers that are prone to degradation.

1.1. Design criterion

The performance of existing mitigation measures in railway transition zones has been evaluated in various ways in the literature. The methods used to evaluate the performance of these measures include numerical simulations, field measurements, material testing, dynamic track testing, and inspection. The effectiveness of these methods in evaluating the performance of mitigation measures is dependent on the choice of performance evaluation criterion. The most common dynamic responses that have been used for assessment of the railway transition zones are vertical displacements and accelerations for rail [19,20] and/or sleepers, vertical stresses in ballast or/and subgrade or/and the stress at sleeper-ballast interface [3,6,12]. In [21], authors have performed a systematic analysis and studied the dynamic responses of the track components in terms of displacements, accelerations, Von Mises stress and mechanical energy, and proposed a design criterion to minimize the amplified degradation of railway transition zones. It was claimed [21] that minimizing the magnitude of total strain energy will imply lesser permanent deformation and hence reduced operation-induced degradation, and the total strain energy being as uniform as possible along the longitudinal direction (i.e., without an abrupt increase or decrease) will minimize non-uniform degradation. The evaluation of the extensively used mitigation measures in railway transition zones (the first aim of the paper as mentioned above), namely approach slabs and transition wedges, will be conducted using this recently developed criterion and the most widely investigated responses (vertical rail displacement and stress in ballast layer) in literature.

1.2. Current design solutions

The approach slabs [19,20,22–26] are most commonly used in areas (the Netherlands) with either soft or highly compressible soils, while transition wedges are used in areas (Spain, Portugal) with either stiffer or less compressible soils. Some numerical simulations [27–31] show that the transition wedges are effective in mitigating transition effects but site measurements contradict these claims [1,2]. A case study [2] reports an exponential degradation of the approach wedge one year after its installation, and differential settlements were comparable to the pre-installation of the wedge. Another case study cite12 relating to a culvert transition with an inclined approach slab shows that the settlement of the subgrade under the slab activates an additional degradation mechanism being the sliding of particles over the inclined plate. In addition to this, the study also reported high degradation close to the extremities of the slab. Moreover, generally speaking, an assessment of the long-term performance of the mentioned mitigation measures is missing in the literature. Hence, there is no strong evidence supporting the effectiveness of these two most commonly used mitigation measures and the reasons behind the ineffectiveness are still not clear.

1.3. New Design (SHIELD)

The above-mentioned new design of a transition structure (the second aim of the paper) is proposed to guide energy away from the trackbed layers that are prone to degradation so as to avoid energy concentrations inside these layers in the vicinity of the transition interface. The authors in [18] have demonstrated that avoiding energy concentrations in the vicinity of the

transition interface mitigates the local dynamic amplifications (no abrupt increase within trackbed layers) in the approach zone. Thus, the geometry of SHIELD has been optimized to guide energy away from the track. In essence, SHIELD aims to minimize the total strain energy in approach zones (implying lesser degradation) and to avoid any local operation-induced amplification in total strain energy that could contribute to the processes leading to hanging sleepers. Consequently, SHIELD provides an effective solution to the challenges of managing energy flow at railway transition zones. The ideal 3-dimensional geometry of SHIELD resembles, in fact, a hull shape. However, in this paper, the effectiveness of this mitigation concept will be evaluated, and for that reason, only the 2-dimensional (2-D) plane is considered. It is to be noted that SHIELD is not designed to counteract autonomous settlements, and additional measures may be needed for the optimal performance of SHIELD to deal with these situations (see Section 4). At the same time, the material properties of SHIELD have been optimized to ensure a gradual increase in equivalent track stiffness.

In this paper, the detailed investigation of existing designs of transition structures, namely approach slabs (horizontal and inclined) and a transition wedge, will therefore be performed using a 2-D finite element model (details in Section 2). The rail deformations, equivalent Von Mises stress and total strain energy in track bed layers will be compared for different scenarios, and the efficiency of these transition structures will be evaluated. In the end, the efficiency of the new design of the transition structure will be demonstrated in terms of the quantities mentioned above. All transition structures studied in this work are simulated with conditions for the most efficient performance. The approach slabs are modelled such that there is no rigid body rotation, the under-sleeper pads are tuned such that there are uniform static displacements throughout the system and the material geometry used for the transition wedge is chosen to deliver the best performance in the conditions under study. In summary, the inefficiency of the mitigation measures due to inappropriate design or installation has been eliminated in this study.

2. Methods

An embankment-bridge transition was simulated using a 2-dimensional plane-strain finite element model (see Figure 1). The model consists of 60 m of the ballasted track (soft side) and 20 m of the ballastless track (stiff side) The ballasted track comprises a beam representing the rail, connected using rail-pads (springs and dashpots) to the sleepers resting on a three-layered substructure. The top layer is 0.3 m of ballast with 1 m each of an embankment (dense sand) and the subgrade (clayey soil) layer underneath. The ballastless track comprises the rail, connected to sleepers with under-sleeper pads resting on a concrete structure with a depth of 2.3 m. A hard contact linear penalty method was used to define the normal behaviour and the Coulomb's friction law was adopted to define the tangential behaviour of the vertical interface between the ballasted and ballastless track. The sleeper (mesh size: 0.03 m), ballast (mesh size: 0.0375 m), embankment (mesh size: 0.0625 m), subgrade (mesh size: 0.0625 m) and the bridge (mesh size: 0.0375 m) were discretized using linear quadrilateral elements of type CPE4R and rail (mesh size: 0.01 m) using two-node linear beam elements of type B21 to form

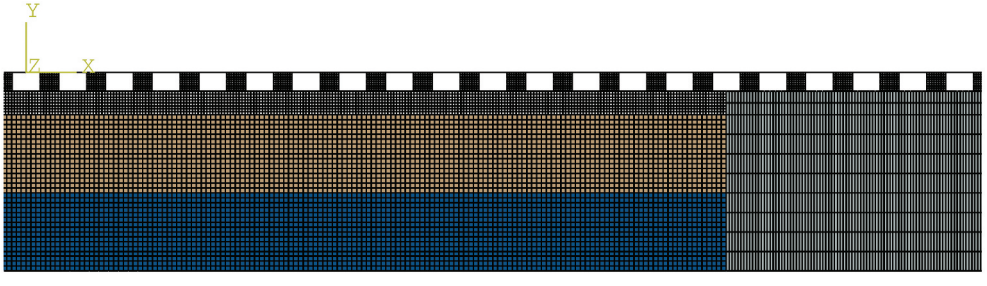

Figure 1. Finite element model of the standard embankment-bridge transition (see Figure 2 for cross-sectional details).

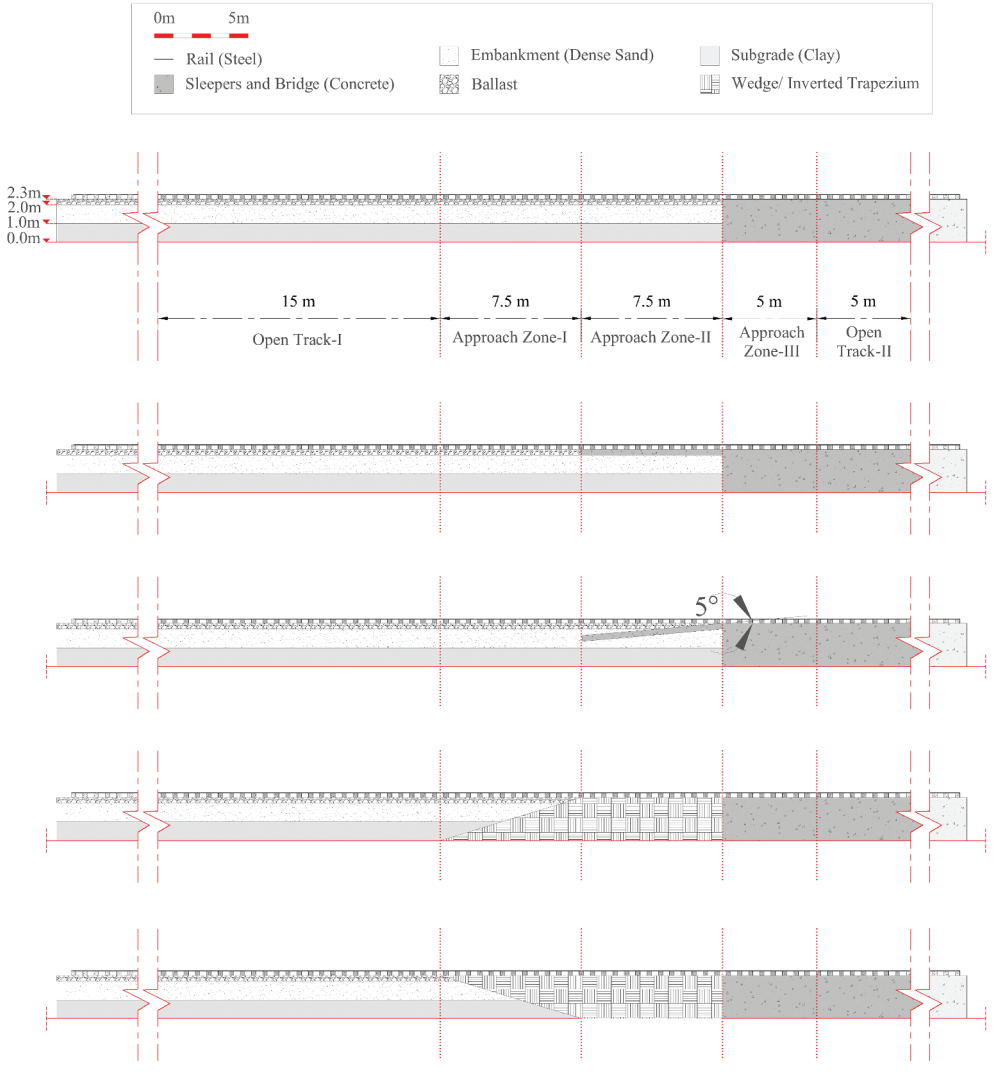

Figure 2. Cross-sectional details of the embankment-bridge transition under study with standard design, horizontal approach slab, inclined approach slab, transition wedge and the new design (in this order from top to bottom).

a regular mesh. The dynamic analysis was performed using implicit scheme time step integration (full Newton-Raphson method) for 1.75 s with a time step of 0.005 s. The details of the model can be found in [21] and the mechanical properties of the material are tabulated in Table 2 [32,33].

The previous paragraph describes the base model which is a standard embankment-bridge transition with no transition structure. The initial validation for this base model regarding the measured vertical rail displacements reported in validation was performed in designCriteria. This model was used to simulate three different types of most commonly used transition structures namely a transition wedge, a horizontal approach slab and an inclined approach slab. Additionally, a new transition structure (SHIELD) with a vertical cross-section of a trapezoid was also studied. Figure 2 shows the longitudinal-section details of these five modelling cases. The five cases studied in this paper are described in detail below. The under-sleeper pads (USP) on the stiff side were tuned such that the static rail deformations remain the same on both the stiff and soft sides of the track. A dynamic analysis with linear elastic material

behaviour was performed using one axle load of 90 kN moving at a speed of 144 km/h for all the cases under study. It is to be noted that the vehicle effects are not accounted for in this work as the main objective is to compare the performance of each mitigation measure under study and capture the main mechanisms governing the dynamic amplifications under the simplest loading conditions and thus in the cleanest possible manner. A sensitivity analysis must be performed for different vehicle speeds, direction of movement and load configurations in order to achieve the most effective implementation of the design solution and this will be addressed in future investigations.

Each model is divided into five zones. Three zones on the soft side and two on the stiff side of the track. The details of these zones can be found in Figure 2 and Table 1. The zones that are affected by transition effects are referred to as the approach zones (AZ-I, AZ-II, AZ-III) and the zones that are unaffected by the transition effects are referred to as open track (OT-I, OT-II).

The responses (as discussed in Section 1) that will be studied for each of the cases mentioned above are:

Table 1. Details of zones under study.

Name of zone	Length (m)	Description
Open track 1 (OT-I)	15	Open track- soft side
Approach Zone 1 (AZ-I)	7.5	Approach zone to transition structure-soft side
Approach Zone 2 (AZ-II)	7.5	Approach zone from transition structure to bridge
Approach Zone 3 (AZ-III)	5	Approach zone-stiff side
Open track 2 (OT-II)	5	Open track- stiff side

Table 2. Mechanical properties of the track components.

Material	Elasticity Modulus E (N/m^2)	Density ρ (kg/m^3)	Poisson's Ratio ν	Rayleigh damping α	Rayleigh damping β
Steel (rail)	21 x 10^{10}	7850	0.3	-	-
Concrete (sleepers)	3.5 x 10^{10}	2400	0.15	-	-
Ballast	1.5 x 10^{8}	1560	0.2	0.0439	0.0091
Sand (embankment)	8 x 10^{7}	1810	0.3	8.52	0.0004
Clay (subgrade)	2.55 x 10^{7}	1730	0.3	8.52	0.0029
USP	1 x 10^{6}	500	0.1	-	-

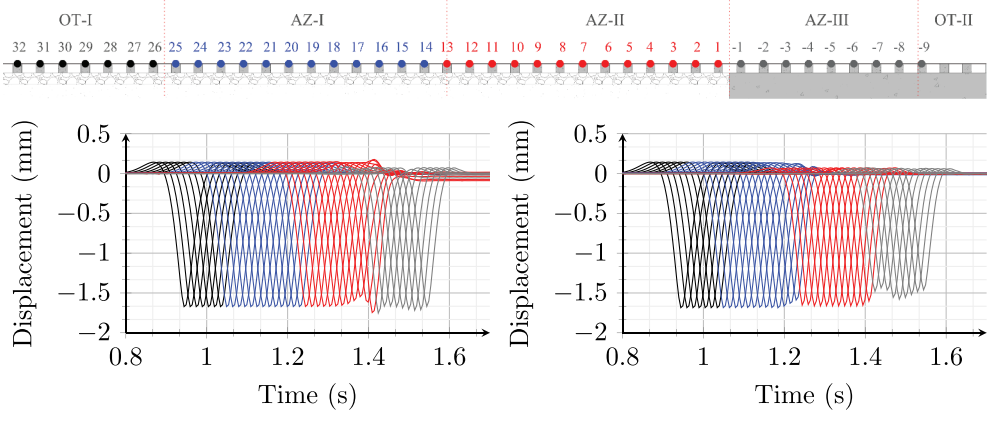

Figure 3. The time history of rail node displacements in OT-I (black), AZ-I (blue), AZ-II (red) and AZ-III (grey) for case 1 (left) and case 2 (right).

Table 3. Mechanical properties of transition wedge and new transition structure.

Transition structure	Elasticity modulus E (N/m^2)	Density ρ (kg/m^3)	Poisson's ratio ν
New design/Wedge	3.6 x 10^8	1900	0.2

- Rail displacements at nodes (see Figure 3) connected to sleepers in OT-I (26 to 30), AZ-I (14 to 25), AZ-II (1 to 14), AZ-III (−1 to −8), OT-II (−9)
- Maximum equivalent Von Mises stress in each zone for ballast.
- Total strain energy (in the volume considered) for each zone (as marked in Figure 2) in the track bed layers (ballast, embankment and subgrade). The strain energy due to only gravity is subtracted from all the results presented in the following sections. It is to be noted that kinetic energy magnitudes are negligible (approximately 10 times smaller) compared to strain energy magnitudes in each layer as shown in designCriteria. Therefore, the total mechanical energy in each layer is dominated by the strain energy.

In [21], the authors concluded that the total strain energy is the most comprehensive quantity to assess the degradation of railway transition zones and proposed an energy-based criterion to evaluate the performance of embankment-bridge transitions. Comparing the above-mentioned responses (incl. displacement, stress and strain energy) for different cases including transition structures, this paper will illustrate the comprehensiveness and robustness of the recently proposed energy criterion for different types of transition zones.

2.1. Case 1 (Standard embankment-bridge transition)

In this case, an embankment-bridge transition is studied without any transition structure to mitigate the dynamic amplifications. This case is used as a benchmark to evaluate the efficiency of currently used mitigation measures presented in cases 2, 3 and 4 and of the newly proposed design presented in case 5. Figure 2 shows the geometrical details of this case.

2.2. Case 2 (Horizontal approach slab)

In this case, a concrete slab of 7.5 m in length and 0.3 m in depth is used as a transition structure which is fixed at the bottom to restrict the rigid body rotation. In this case, the under-sleeper pads on the bridge are tuned such that the static displacements on the bridge are the same as on the approach slab.

2.3. Case 3 (Inclined approach slab)

In this case, an inclined concrete slab of 7.5 m in length and 0.3 m in depth is used as a transition structure. It is inclined at five degrees with the longitudinal direction of the track and is fixed at the bottom to restrict the rigid body motion. The under-sleeper pads on the bridge and the approach slab are tuned similarly to case 2.

2.4. Case 4 (Transition Wedge)

In this case, a wedge-shaped transition structure is used to mitigate the dynamic amplification in the RTZ. The geometric details of the wedge can be seen in Figure 2. The inclined-interface conditions are the same as mentioned above for the vertical transition interface in case 1. The mechanical properties of the wedge can be found in the Table 3.

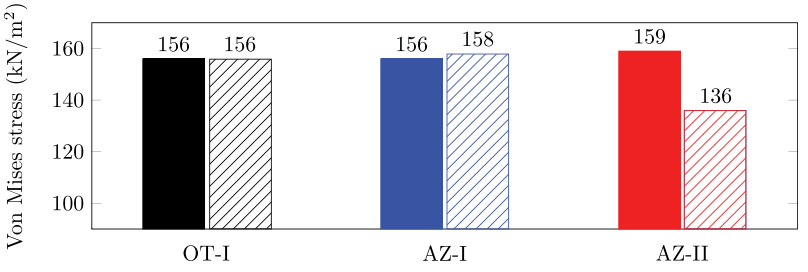

Figure 4. Max. Von Mises stress in the ballast layer in OT-I, AZ-I and AZ-II for case 1 (solid bars) and case 2 (striped bars).

2.5. Case 5 (New design-SHIELD)

In this case, a new concept of design of transition structure is used to mitigate the dynamic amplifications in the RTZ. The behaviour of this transition structure is only studied in the longitudinal and vertical direction in this paper. The vertical cross-section of SHIELD in the longitudinal direction is a trapezoidal-shaped geometry with major base (top) of 15 m length and the minor base (bottom) is 7.5 m long, and other geometric details of the trapezium are given in Figure 2. The mechanical properties of the new transition structure can be found in Table 3.

3. Results and discussion

This section presents the comparison of the standard embankment-bridge transition (case 1) with the horizontal approach slab (case 2), the inclined approach slab (case 3), the transition wedge (case 4), and the railway-transition SHIELD (case 5) with a trapezium-shaped cross-section, in terms of rail displacements, maximum equivalent Von Mises stress and total strain energies for the zones mentioned in Table 1. In addition to these comparative cases, a comparison of the two most promising solutions (case 4 and case 5) is presented at the end.

3.1. Standard embankment-bridge transition (case 1) versus horizontal approach slab (case 2)

3.1.1. Displacements

Figure 3 shows the time history of displacements for locations above the sleepers on the rail in the zones under study for cases 1 and 2. It can be seen that there is an increase in the magnitude of displacement under the load at locations 1 and −1 with respect to OT-I for case 1 but no increase for case 2 in any of the zones under study.

3.1.2. Maximum equivalent Von Mises stress

Figure 4 shows the maximum equivalent Von Mises stress for the ballast layer in OT-I (black), AZ-I (blue) and AZ-II (red) for case 1 and case 2. It can be verified that the increase in the max. Von Mises stress in AZ-II compared to OT-I in case 1 is observed around the transition interface. Although the horizontal approach slab leads to a reduction in the max. Von Mises stress in AZ-II (relative to OT-I), an amplification is seen in AZ-I.

3.1.3. Strain energy

Figure 5 shows a comparison of total strain energy in the layers of ballast (a), embankment (b) and subgrade (c) in the zones shown in Figure 2 for case 1 and case 2. The total strain energy for case 2 in

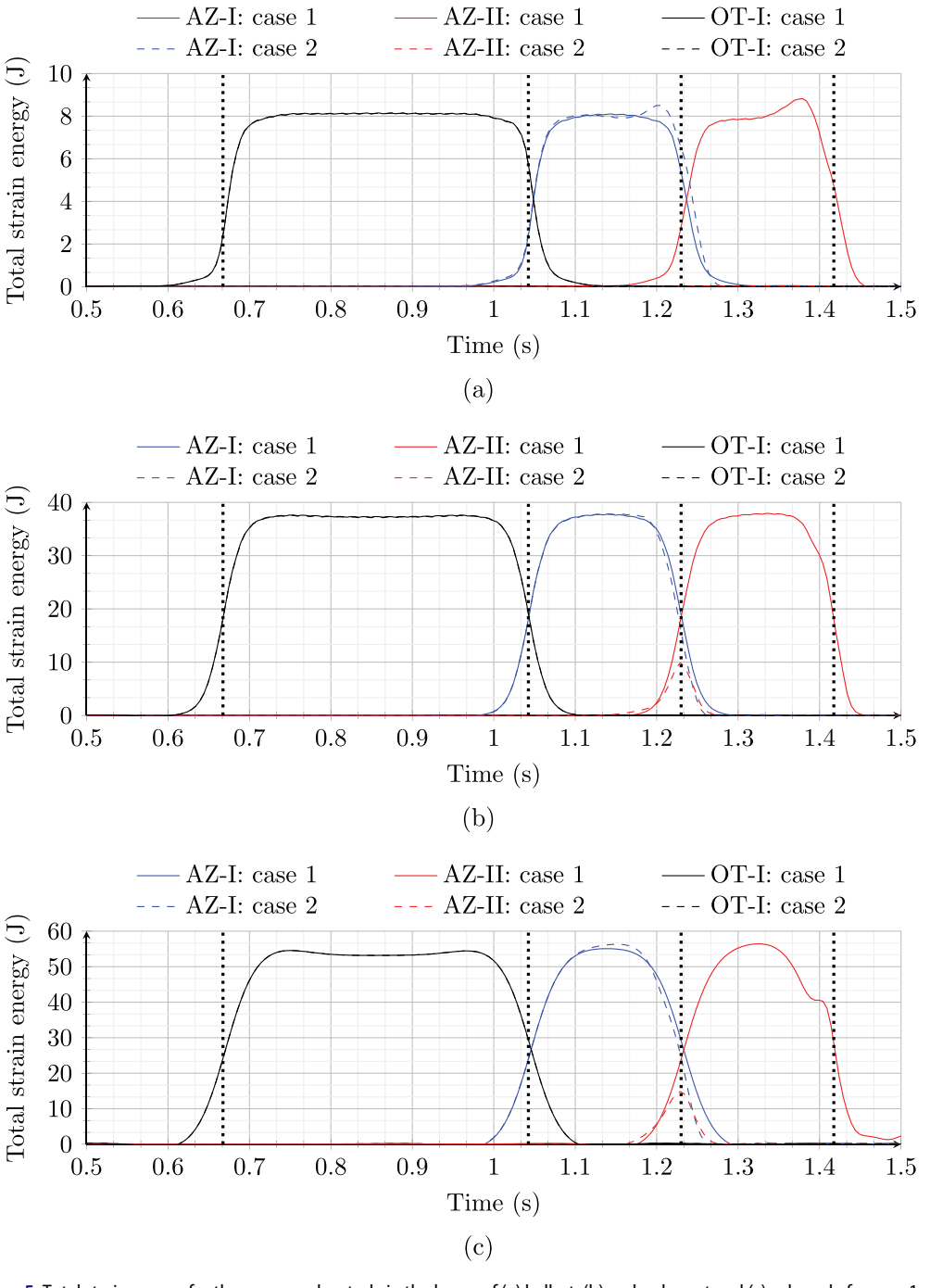

Figure 5. Total strain energy for the zones under study in the layers of (a) ballast, (b) embankment and (c) subgrade for case 1 and case 2. The vertical-dotted lines mark the time moments at which the load enters and exits each of the zones under study.

AZ-II cannot be seen in Figure 5 due to the magnitude being negligible compared to that in the other zones. It is evident from the results that the horizontal approach slab leads to a reduction of the total strain energy (in AZ-II relative to OT-I) in the layers of embankment and subgrade but does not lead to any significant reduction in the ballast layer. The amplification of total strain

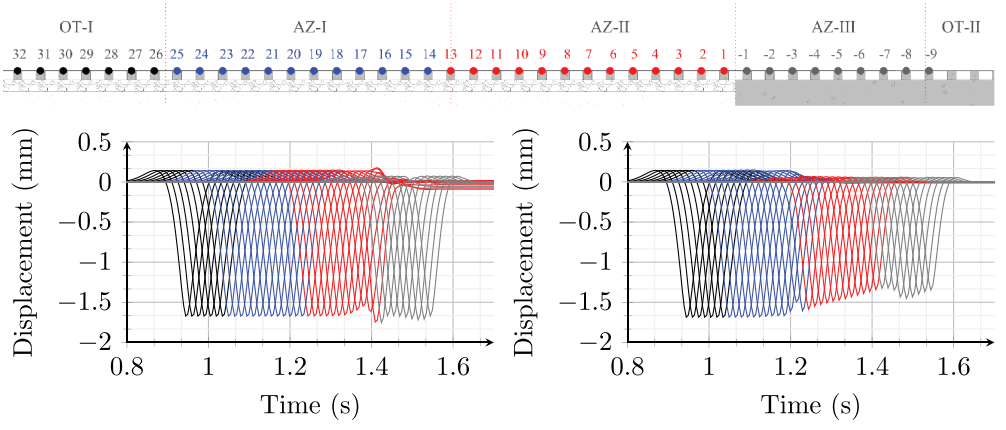

Figure 6. The time history of rail node displacements in OT-I (black), AZ-I (blue), AZ-II (red) and AZ-III (grey) for case 1 (left) and case 3 (right).

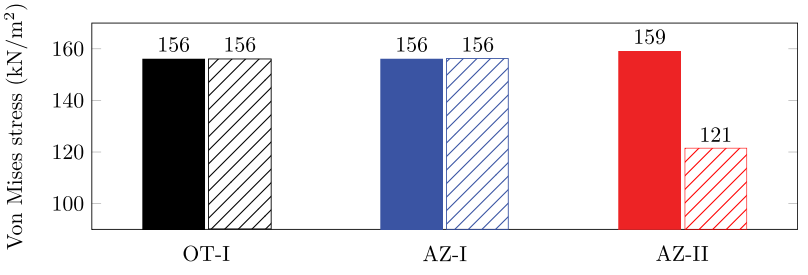

Figure 7. Max. Von Mises stress in the ballast layer in OT-I, AZ-I and AZ-II for case 1 (solid bars) and case 3 (striped bars).

energy in the ballast layer that can be seen in AZ-II for case 1 simply shifts (it only gets slightly smaller) to AZ-I for case 2. This implies that adopting an approach slab creates a new transition zone at the end of the slab instead of mitigating the problem.

It is to be noted that, even though the horizontal approach slab shows no amplification in the kinematic response and only a minor increase in equivalent Von Mises stress, a clear amplification of the strain energy in the ballast layer is observed. The fact that the displacement decreases does not necessarily mean that the associated stress or the strain energy (combination of stress and strain) also diminishes. The strain energy amplification most clearly explains the inefficiency of this particular transition structure.

3.2. Standard embankment-bridge transition (case 1) versus inclined approach slab (case 3)

3.2.1. Displacements

Figure 6 shows the time history of displacements for locations above the sleepers on the rail in the zones under study for case 1 and case 3. The results shown on the left in Figure 6 are the same as shown previously. For case 3 the displacements are observed to reduce gradually in AZ-II compared to those in case 1.

3.2.2. Maximum equivalent Von Mises stress

Figure 7 shows the maximum equivalent Von Mises stress for the ballast layer in OT-I (black), AZ-I (blue) and AZ-II (red) for case 1 and case 3. Compared to case 1 and case 2 that both

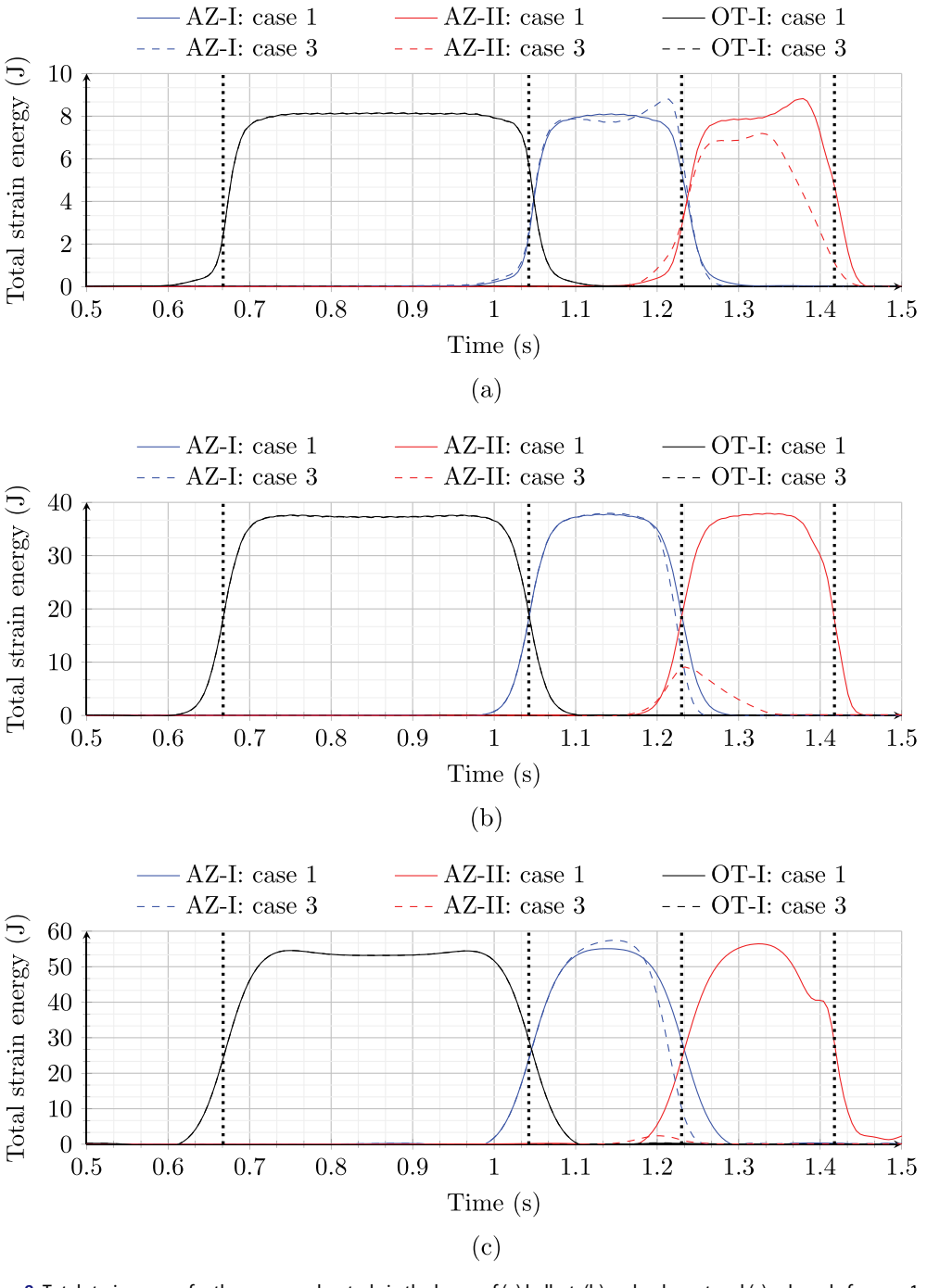

Figure 8. Total strain energy for the zones under study in the layers of (a) ballast, (b) embankment and (c) subgrade for case 1 and case 3. The vertical-dotted lines mark the time moments at which the load enters and exits each of the zones under study.

showed an increase in max. Von Mises stress in AZ-II and AZ-I, respectively, relative to OT-I, there is no amplification in stress for any of the zones under study for case 3. Moreover, there is a reduction in AZ-II for case 3 similar to what is observed for case 2, but the amount of reduction is higher.

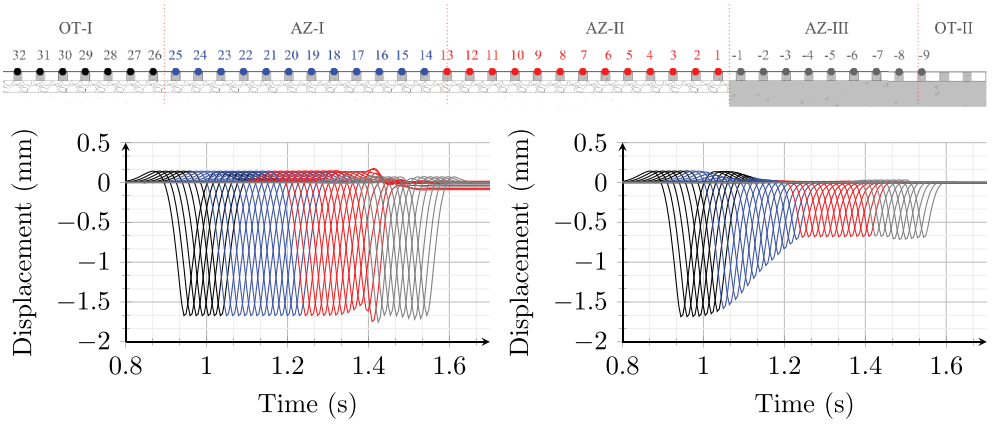

Figure 9. The time history of rail node displacements in OT-I (black), AZ-I (blue), AZ-II (red) and AZ-III (grey) for case 1 (left) and case 4 (right).

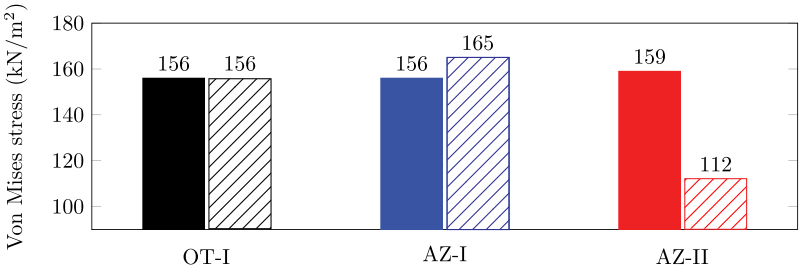

Figure 10. Max. Von Mises stress in the ballast layer in OT-I, AZ-I and AZ-II for case 1 (solid bars) and case 4 (striped bars).

3.2.3. Strain energy

Figure 8 shows a comparison of total strain energy in the layers of ballast (a), embankment (b) and subgrade (c) for the zones shown in Figure 2, for case 1 and case 3. The total strain energy in all three track-bed layers in OT-I is the same for both the cases under study as expected. The total strain energy shows a peak in AZ-I for case 3 which is the same in magnitude as the peak observed for case 1 in AZ-II. Like for case 2, this implies that the transition effects are simply shifted but not mitigated by using an inclined approach slab. Moreover, a small increase in the total strain energy is also observed for the subgrade layer in case 3 compared to case 1. In summary, the use of an inclined approach slab could not reduce the dynamic amplifications in the RTZ under study but made it worse. It is important to highlight that the inclined approach slab seemed to be an efficient solution when evaluated using the kinematic response or the stress distribution as a criterion. However, the energy criterion clarifies the reason behind the inefficiency of this particular transition structure in reality.

3.3. Standard embankment bridge transition (case 1) versus transition wedge (case 4)

3.3.1. Displacements

Figure 9 shows the time history of displacements for locations above the sleepers on the rail in the zones under study for case 1 and case 4. As mentioned above, the displacement at locations 1 and −1 for case 1 exhibits an increase, as is evident from the observation, but for case 4 the displacements gradually decrease in AZ-I and becomes constant in AZ-II and AZ-III. No abrupt changes were

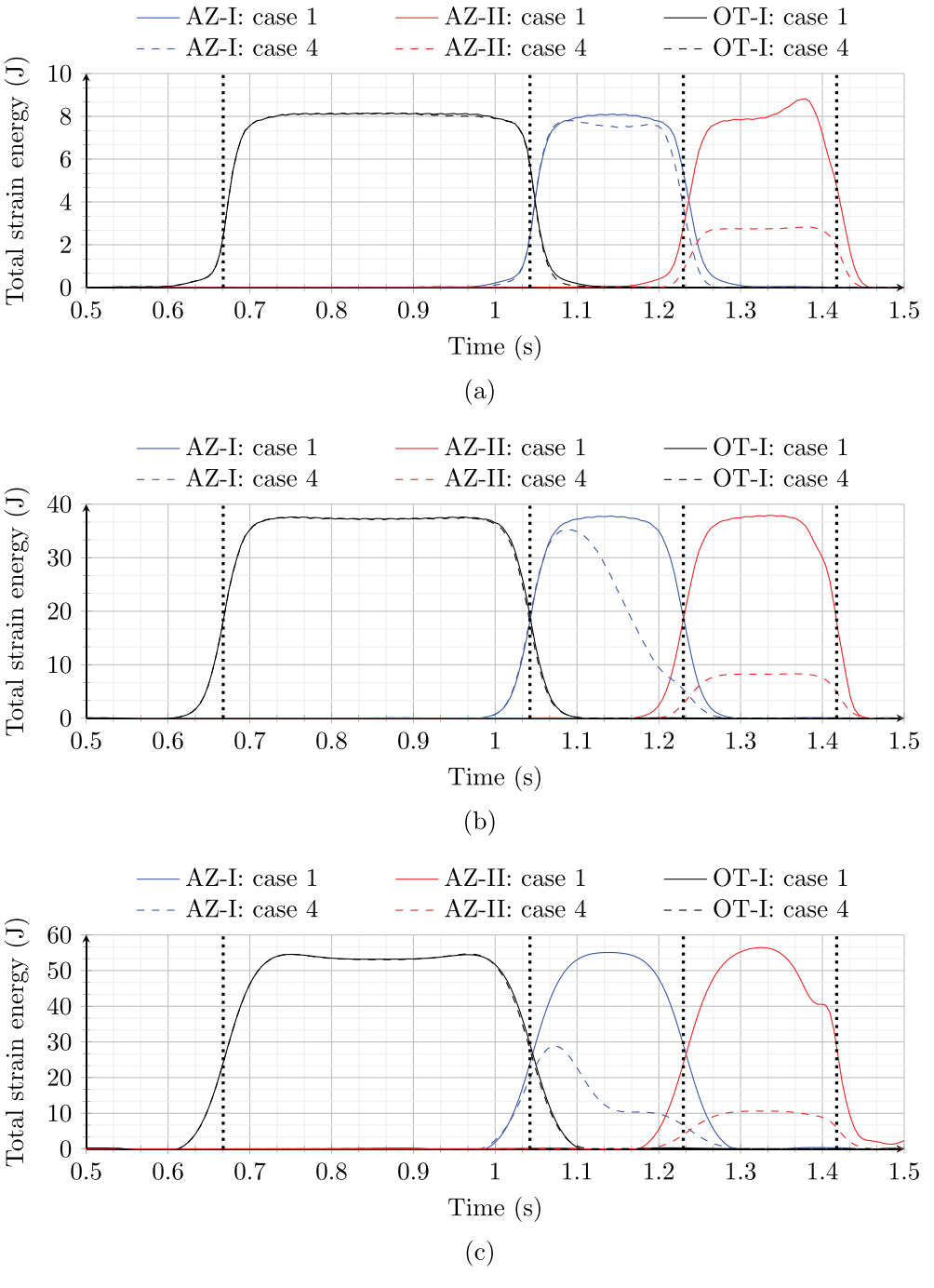

Figure 11. Total strain energy for the zones under study in the layers of (a) ballast, (b) embankment and (c) subgrade for case 1 and case 4. The vertical-dotted lines mark the time moments at which the load enters and exits each of the zones under study.

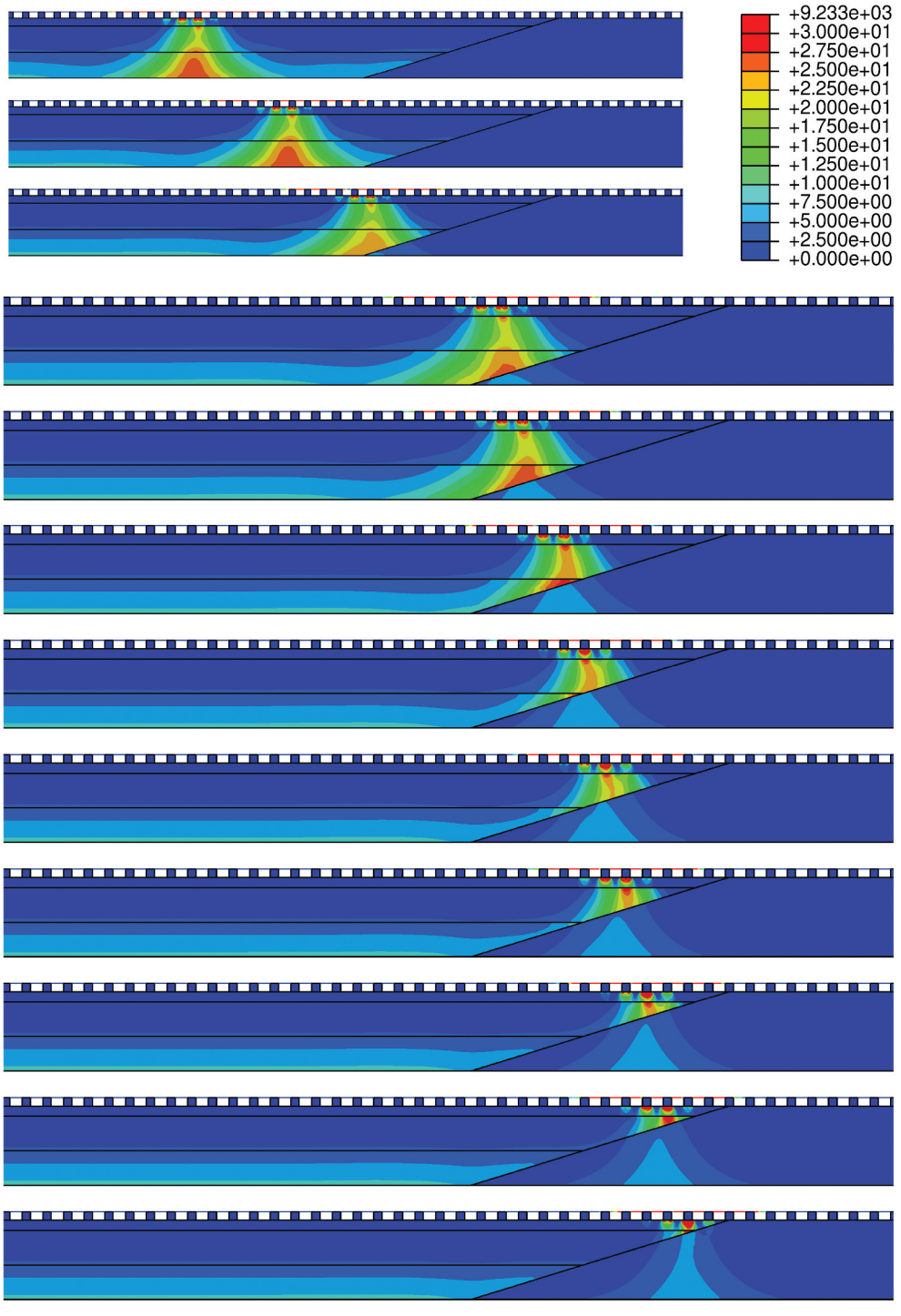

Figure 12. Contour plot of the strain energy in the system as the load approaches the transition wedge. Snapshots for time moments (from top to bottom) 0.8841 s, 0.9741 s, 1.049 s, 1.064 s, 1.079 s, 1.109 s, 1.129 s, 1.144 s, 1.154 s, 1.174 s, 1.184 s, 1.204 s.

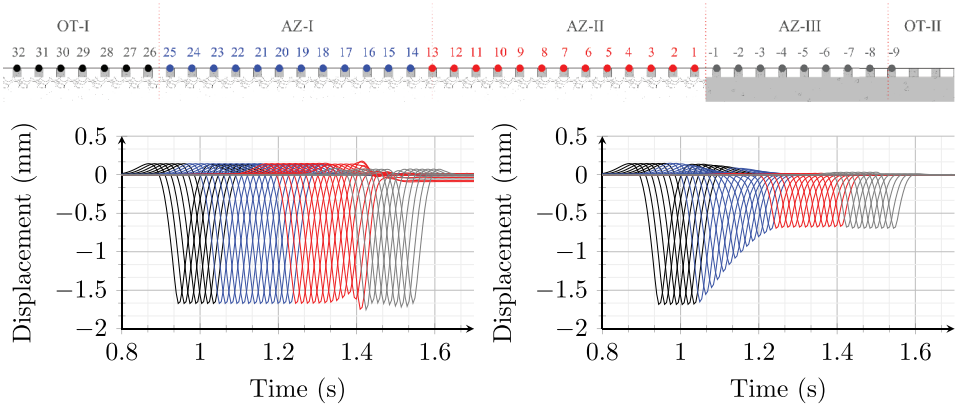

Figure 13. The time history of rail node displacements in OT-I (black), AZ-I (blue), AZ-II (red) and AZ-III (grey) for case 1 (left) and case 5 (right).

observed in any of the zones under study. Hence, the transition wedge seems to be a promising solution if the performance is evaluated solely based on vertical rail displacements.

3.3.2. Maximum equivalent Von Mises stress

Figure 10 shows the maximum equivalent Von Mises stress for the ballast layer in OT-I (black), AZ-I (blue) and AZ-II (red) for case 1 and case 4. Although the displacement fields looks ideal for case 4, it can be verified that the Von Mises stress distribution across the zones is non-uniform and increases in AZ-I relative to OT-I (and then reduces again in AZ-II). This increase in stress indicates that the transition effects are not mitigated by the transition wedge but only moved further (on the soft side) from the previous location, like in case 1. The increase in case 4 is much higher than that observed in case 1 (compare Figures 4 and 10), implying that the response is worse with this particular transition structure.

3.3.3. Strain energy

Figure 11 shows a comparison of total strain energy in the layers of ballast (a), embankment (b) and subgrade (c) for the zones shown in Figure 2 for case 1 and case 4. The transition wedge used in case 4 shows a significant reduction in total strain energy in the layers of embankment and subgrade. However, the total strain energy in the layer of ballast shows an increase towards the end of AZ-I compared to Figure 15(a), where it smoothly decreases as a result of the added specific transition structure which provides the same change in overall (static) tracks stiffness as the current wedge structure. Although the magnitude of total strain

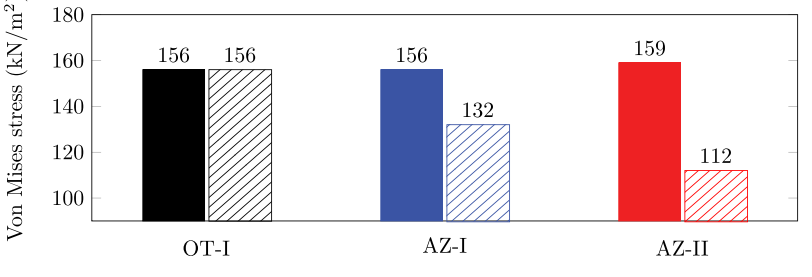

Figure 14. Max. Von Mises stress in the ballast layer in OT-I, AZ-I and AZ-II for case 1 (solid bars) and case 5 (striped bars).

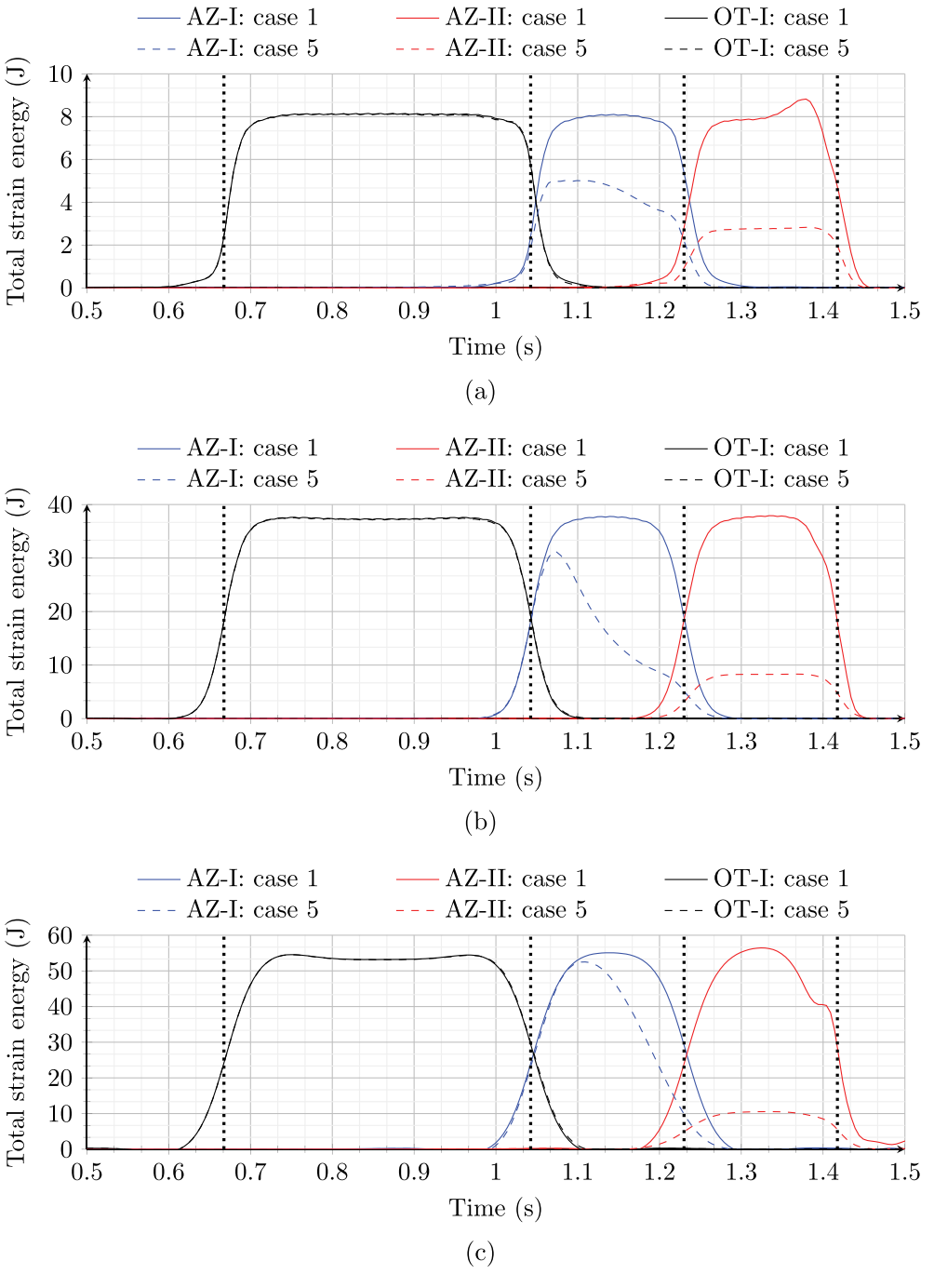

Figure 15. Total strain energy for the zones under study in the layers of (a) ballast, (b) embankment and (c) subgrade for case 1 and case 4. The vertical-dotted lines mark the time moments at which the load enters and exits each of the zones under study.

energy in AZ-I and AZ-II is less compared to the standard embankment-bridge transition (case 1), the reduction in AZ-I is not significant considering that the overall stiffness of this zone has increased considerably compared to OT-I which ideally should lead to a significant reduction in strain energy similar to case 5, as discussed in following sections. The

inefficiency of the transition wedge can be attributed to guiding of strain energy (see Figure 12) from the bottom layers to the ballast layer due to the unfavourable geometry. The response will amplify even more in case of imperfections in the track, as demonstrated in Section 3.5.

3.4. Standard embankment bridge transition (case 1) versus new design: SHIELD (case 5)

3.4.1. Displacements

Figure 13 shows the time history of displacements for locations above the sleepers on the rail in the zones under study for case 1 and case 5. Observing the results, it is apparent that the time history of displacements shows a resemblance to the case with a transition wedge due to the overall (static) track stiffness being the same. The displacements under the load gradually decrease in AZ-I, and becomes constant in AZ-II and AZ-III, and no abrupt changes were observed in any of the zones under study.

3.4.2. Maximum equivalent Von Mises stress

Figure 14 shows the maximum equivalent Von Mises stress for the ballast layer in OT-I (black), AZ-I (blue) and AZ-II (red) for case 1 and case 5. Case 5, which includes the new design of transition structure, demonstrates a gradual decrease in max. Von Mises stress in AZ-I and AZ-II relative to OT-I. No amplification is observed in any of the zones under study for case 5, unlike all the cases studied above. This indicates that the behaviour is promising, but the energy analysis (below) should obviously confirm that before conclusions can be drawn.

3.4.3. Strain energy

Figure 15 shows a comparison of total strain energy in the layers of ballast (a), embankment (b) and subgrade (c) for the zones shown in Figure 2 for case 1 and case 5. It is evident from the results that the new design leads to a gradual decrease in total strain energy in all three track-bed layers. No peaks are observed in AZ-I and AZ-II, and the magnitudes are much lower than in OT-I. Case 5 shows a significant reduction in the magnitude of the total strain energy in AZ-I and AZ-II relative to OT-I in the layers of ballast and embankment compared to all the cases with existing mitigation measures. In the subgrade layer, case 4 Figure 15(c) shows more reduction in total strain energy compared to case 5 in AZ-I. However, this can be attributed to the larger volume of stiffer material in AZ-I in case 4 compared to case 5, as the strain energy density is typically smaller for stiffer materials. In any case, SHIELD shows no amplification in any of the zones or layers under study and guides energy away from the upper track bed layers as seen in Figure 16. This is exactly the reason as to why case 5 outperforms case 4 (Figure 12), where the energy is guided towards the upper track bed layers, which leads to an energy concentration.

3.5. Transition wedge (case 4) versus SHIELD of railway transition zone (case 5)

Figure 17 summarizes the comparison of case 4 and case 5 in terms of equivalent stiffness (static) in AZ-I, rail displacements, equivalent Von-Mises stress and total strain energies. Figure 17(a) shows a gradual increase (same for case 4 and case 5) in equivalent trackbed stiffness from OT-I to AZ-II. Figure 17(b) shows a gradual decrease in rail displacements in AZ-I which is same for both case 4 and case 5. However, the equivalent Von Mises stress Figure 17(c) in AZ-I for case 4 is much higher than case 5 due to reasons discussed in Section 3.3, and this can be also seen in strain energy Figure 17(d) that combines the stress and strain fields over a volume. On one hand, despite a significant increase in stiffness, the max. Von Mises stress and the total strain energy in the AZ-I for the case with the transition wedge show no significant improvement in the ballast layer. On the other hand, case 5 shows a gradual decrease in Von Mises stress and total strain energy in AZ-I. Although case 4 shows no

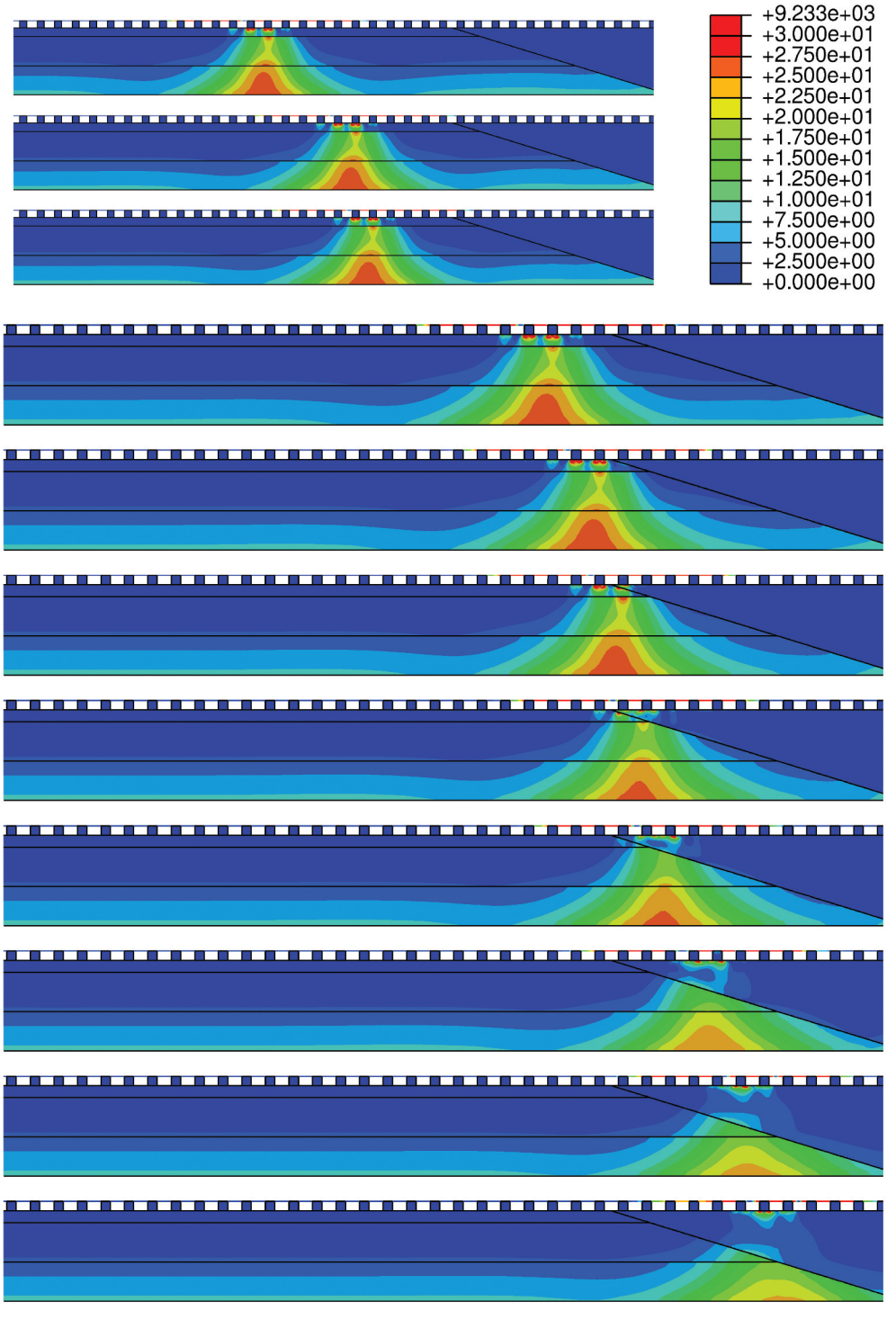

Figure 16. Contour plot of the strain energy in the system as the load approaches the new transition structure: SHIELD. Snapshots for time moments (from top to bottom) 0.8841 s, 0.9591 s, 0.9741 s, 1.004 s, 1.034 s, 1.049 s, 1.064 s, 1.079 s, 1.109 s, 1.134 s, 1.149 s.

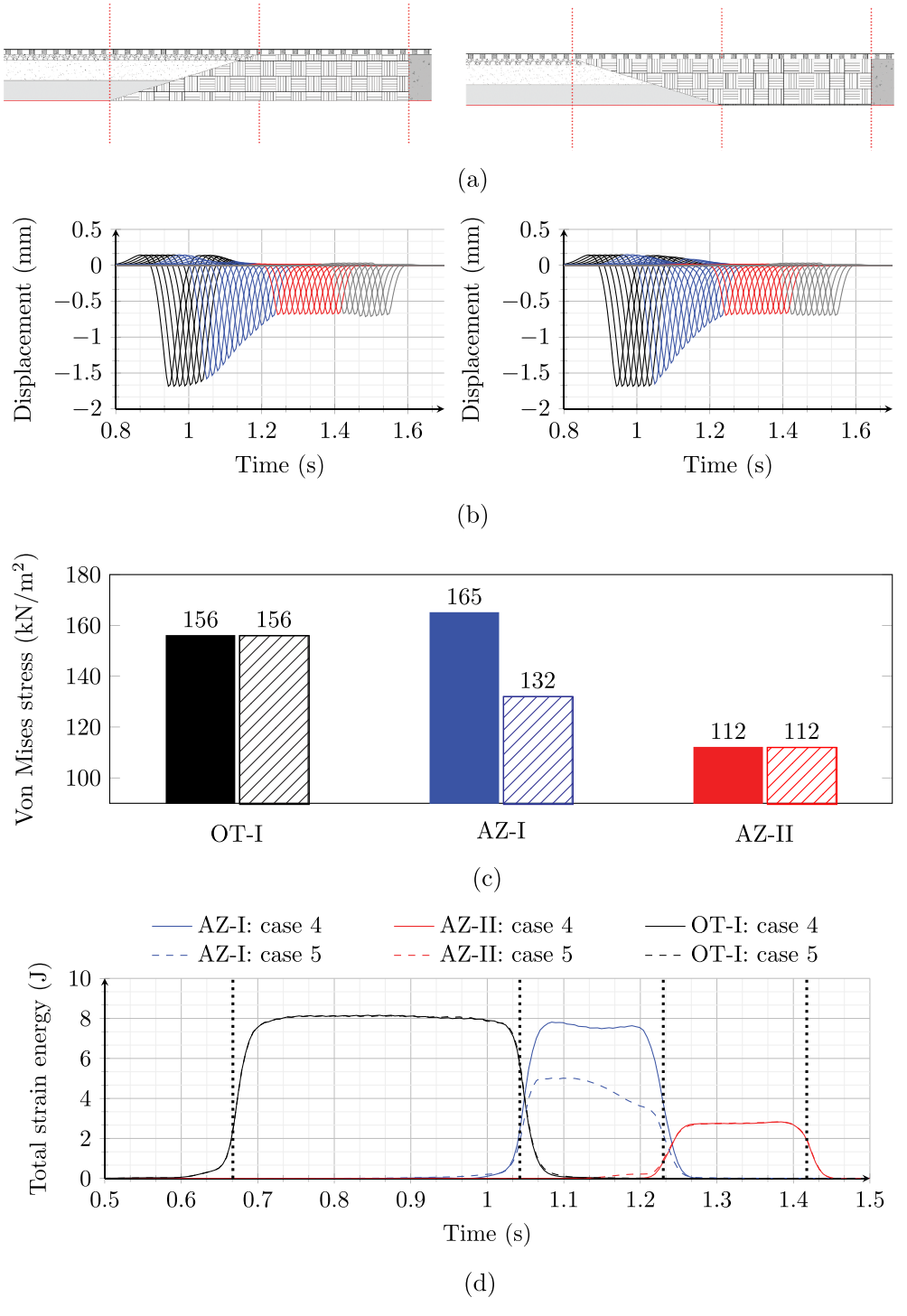

Figure 17. (a) cross-section details, (b) comparison of rail displacements for case 4 (left) and case 5 (right), (c) equivalent Von Mises stress and (d) time history of total strain energy.

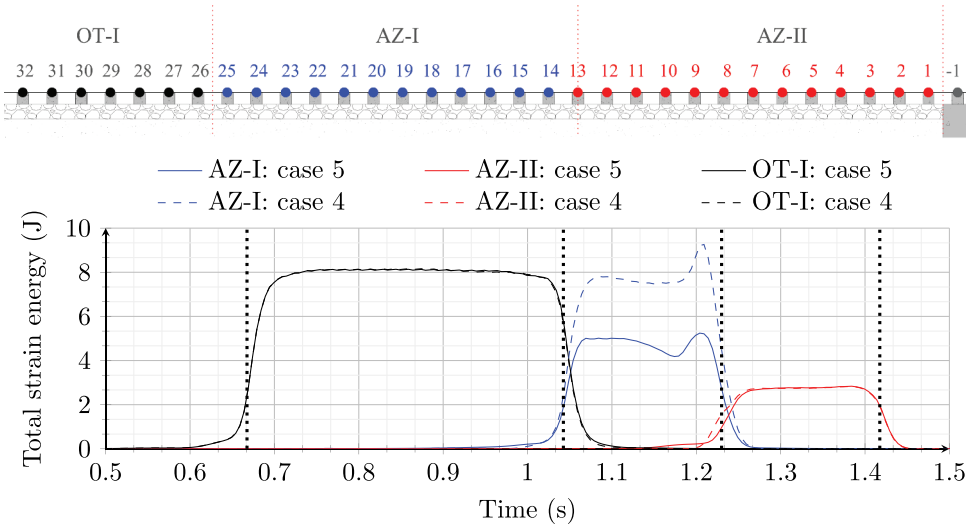

Figure 18. Total strain energy for the zones under study in the ballast layer for case 4 and case 5 accounting for the loss of contact under sleeper 15 in AZ-I for both the cases. The vertical-dotted lines mark the time moments at which the load enters and exits each of the zones under study.

amplification in the total strain energy in AZ-I with respect to OT-I, it can be verified that the total strain energy increases locally in the proximity of interface between AZ-I and AZ-II in the ballast layer. Moreover, Figure 12 shows that the strain energy is guided towards the upper layers leading to an increase due to the unfavourable geometry of the transition wedge. This increase in strain energy can be worse in case of an imperfection along the track in this zone. Thus, in this section, the total strain energy for cases 4 and 5 will be compared to evaluate their performances in a non-ideal condition, i.e., a contact loss under sleeper 15 in AZ-I (refer to Figure 18 for the location of this sleeper) for case 4 and case 5.

Figure 18 shows the comparison of the total strain energy (OT-I, AZ-I, AZ-II) between case 4 and case 5 in the ballast layer under the non-ideal condition for both the cases. The total strain energy in the embankment and subgrade layers are not shown as amplifications due to the lost contact between sleeper 15 and the ballast layer are observed only in the ballast layer. Indeed, a significant amplification of total strain energy can be seen in AZ-I for case 4. A similar amplification takes place for case 5, but it is not high enough to exceed the energy level in OT-I. Hence, it is concluded that the case 5 outperforms case 4 not only in ideal conditions (Section 3.3 and Section 3.4) but especially in a non-ideal condition.

4. Conclusions

A comprehensive evaluation of existing transition structures and a new safe hull-inspired energy limiting design (SHIELD) for railway transition zones was performed.

Firstly, the existing transition structures, namely horizontal approach slab, inclined approach slab and transition wedge, were evaluated in terms of the most commonly studied responses (vertical rail displacement and stress in ballast) and the recently developed criterion based on total strain energy. None of the cases with transition structures led to local amplification in vertical rail displacements in the proximity of the transition interface, while the standard embankment-bridge transition case (with no transition structure) does. The maximum Von Mises stress in the zones under study showed a reduction for the cases with approach slabs (both horizontal and

inclined) but an increase for the case with a transition wedge. In the end, looking at the total strain energy, which is the most comprehensive response quantity (and therefore the best damage indicator), a clear amplification was seen for all existing transition structures, which indicates the poor performance of these existing transition structures.

The second part of the paper evaluates the newly introduced transition structure (SHIELD) using the same criterion as used for the evaluation of the existing transition structures. The results presented in Section 3 make it evident that there is a gradual decrease in vertical rail displacements, max. equivalent Von Mises stress and, most importantly, in the total strain energy when moving from the open track to the transition interface. No local amplification was observed in any of the approach zones and, in addition to this, the magnitudes of all the responses were much lower than those in all other cases studied in this paper. Furthermore, the transition wedge was clearly outperformed by SHIELD under non-ideal conditions (loss of contact under the sleepers). Even though the SHIELD performs well under non-ideal conditions and is capable of dealing with consequences of autonomous settlement to some extent, it can be also combined with measures like adjustable sleepers [12] or wedge-shaped sleepers [13] to avoid loss of contact due to non-uniform settlement and reduce the maintenance requirements even more.

Future investigations related to this newly proposed transition structure must include the influence of the vehicle-structure interactions, three-dimensional response, material and geometric parameter sensitivities and experimental validation to lay out the guidelines regarding the choice of the parameters for effective and robust solutions.

Disclosure statement

No potential conflict of interest was reported by the author(s).

Funding

This research is supported by the Dutch Technology Foundation TTW (Project 15968), a part of the Netherlands Organisation for Scientific Research (NWO), and which is partly funded by the Ministry of Economic Affairs.

References

[1] Indraratna B, Sajjad MB, Ngo T, et al. Improved performance of ballasted tracks at transition zones: a review of experimental and modelling approaches. Transp Geotech. 2019;21:100260. doi: 10.1016/j.trgeo.2019.100260

[2] Sañudo R, dellOlio L, Casado J, et al. Track transitions in railways: a review. Constr Build Mater. 2016;112:140–157. doi: 10.1016/j.conbuildmat.2016.02.084

[3] Wang H, Chang L, Markine V. Structural health monitoring of railway transition zones using satellite radar data. Sensor. 2018;18(2):413. doi: 10.3390/s18020413

[4] Fortunato E, Paixão A, Calçada R. Railway track transition zones: design, construction, monitoring and numerical modelling. Int J Railw Tech. 2013;2(4):33–58. doi: 10.4203/ijrt.2.4.3

[5] Namura A, Suzuki T. Evaluation of countermeasures against differential settlement at track transitions. Q Report Rtri. 2007;48(3):176–182. doi: 10.2219/rtriqr.48.176

[6] Shang Y, Nogal M, Wang H, et al. Systems thinking approach for improving maintenance management of discrete rail assets: a review and future perspectives. Struct Infrastruct Eng. 2021;19(2):197–215. doi: 10.1080/15732479.2021.1936569

[7] Bizjak KF, Knez F, Lenart S, et al. Life-cycle assessment and repair of the railway transition zones of an existing bridge using geocomposite materials. Struct Infrastruct Eng. 2017;13(3):331–344. doi: 10.1080/15732479.2016.1158288

[8] Ribeiro CA, Paixão A, Fortunato E, et al. Under sleeper pads in transition zones at railway underpasses: numerical modelling and experimental validation. Struct Infrastruct Eng. 2015;11(11):1432–1449. doi: 10.1080/15732479.2014.970203

[9] Heydari-Noghabi H, Varandas JN, Esmaeili M, et al. Investigating the influence of auxiliary rails on dynamic behavior of railway transition zone by a 3d train-track interaction model. Latin Am J Solid Struct. 2017;14(11):2000–2018. doi: 10.1590/1679-78253906
[10] Fărăgău A, Jain A, de Oliveira Barbosa J, et al. Auxiliary rails as a mitigation measure for degradation in transition zones. In: Pombo J, editor. Proceedings of The Fifth International Conference on Railway Technology: Research, Development and Maintenance; (Civil-Comp Conferences; Vol. 1); United Kingdom: Civil-Comp Press; 2023.
[11] Esmaeili M, Heydari-Noghabi H, Kamali M. Numerical investigation of railway transition zones stiffened with auxiliary rails. Proc Instit Civil Engin Trans. 2020;173(5):299–308. doi: 10.1680/jtran.17.00035
[12] Wang H, Markine V. Corrective countermeasure for track transition zones in railways: adjustable fastener. Eng Struct. 2018;169:1–14. doi: 10.1016/j.engstruct.2018.05.004
[13] Jia W, Markine V, Carvalho M, et al. Design of a concept wedge-shaped self-levelling railway sleeper. Constr Build Mater. 2023;386:131524. doi: 10.1016/j.conbuildmat.2023.131524
[14] Chumyen P, Connolly D, Woodward P, et al. The effect of soil improvement and auxiliary rails at railway track transition zones. Soil Dyn Earthquake Eng. 2022;155:107200. doi: 10.1016/j.soildyn.2022.107200
[15] Hu P, Zhang C, Wen S, et al. Dynamic responses of high-speed railway transition zone with various subgrade fillings. Comput Geotech. 2019;108:17–26. doi: 10.1016/j.compgeo.2018.12.011
[16] Punetha P, Nimbalkar S. An innovative rheological approach for predicting the behaviour of critical zones in a railway track. Acta Geotech. 2023;18(10):5457–5483. doi: 10.1007/s11440-023-01888-3
[17] Selig ET, Li D Track modulus: its meaning and factors influencing it. Transportation Research Record. 1994; Available from: http://onlinepubs.trb.org/Onlinepubs/trr/1994/1470/1470-006.pdf.
[18] Jain A, Metrikine A, Steenbergen M, et al. Dynamic amplifications in railway transition zones: investigation of key phenomena. Journal of Physics: Conference Series; Delft, Netherlands. IOP Publishing; 2023.
[19] Heydari-Noghabi H, Zakeri J, Esmaeili M, et al. Field study using additional rails and an approach slab as a transition zone from slab track to the ballasted track. Proc Inst Mech Eng F J Rail Rapid Transit. 2017;232(4):970–978. doi: 10.1177/0954409717708527
[20] Asghari K, Sotoudeh S, Zakeri JA. Numerical evaluation of approach slab influence on transition zone behavior in high-speed railway track. Transp Geotech. 2021;28:100519. doi: 10.1016/j.trgeo.2021.100519
[21] Jain A, Metrikine AV, Steenbergen MJMM, et al. Design of railway transition zones: a novel energy-based criterion; 2023. Available from: https://arxiv.org/abs/2310.07956.
[22] Varandas J, Hölscher P, Silva M. Three-dimensional track-ballast interaction model for the study of a culvert transition. Soil Dyn Earthquake Eng. 2016;89:116–127. doi: 10.1016/j.soildyn.2016.07.013
[23] Laco K, Borzovič V. Reliability of approach slabs and modelling of transition zones of bridges. Appl Mech Mater. 2016;821:741–746. doi: 10.4028/www.scientific.net/AMM.821.741
[24] Ognibene G, Powrie W, Pen LL, et al. Analysis of a bridge approach: long-term behaviour from short-term response. In: 15th Railway Engineering Conference, Edinburgh, U.K. July; 2019. p. 1–15.
[25] Coelho BZ, Hicks MA. Numerical analysis of railway transition zones in soft soil. Proc Inst Mech Eng F J Rail Rapid Transit. 2015;230(6):1601–1613. doi: 10.1177/0954409715605864
[26] Sakhare A, Farooq H, Nimbalkar S, et al. Dynamic behavior of the transition zone of an integral abutment bridge. Sustainability. 2022;14(7):4118. doi: 10.3390/su14074118
[27] Paixão A, Fortunato E, Calçada R. A numerical study on the influence of backfill settlements in the train/track interaction at transition zones to railway bridges. Proc Inst Mech Eng F J Rail Rapid Transit. 2015;230(3):866–878. doi: 10.1177/0954409715573289
[28] Paixão A, Fortunato E, Calçada R. Design and construction of backfills for railway track transition zones. Proc Inst Mech Eng F J Rail Rapid Transit. 2013;229(1):58–70. doi: 10.1177/0954409713499016
[29] Palomo ML, Martnez JHA, Arnoa AZ, et al. Structural and vibration performance in different scenarios of a prefabricated wedge for railway transition zones. J Vib Eng Technol. 2021;9(7):1657–1668. doi: 10.1007/s42417-021-00319-5
[30] Ribeiro CA, Calçada R, Delgado R. Calibration and experimental validation of a dynamic model of the train-track system at a culvert transition zone. Struct Infrastruct Eng. 2017;14(5):604–618. doi: 10.1080/15732479.2017.1380674
[31] Paixão A, Fortunato E, Calçada R. Transition zones to railway bridges: track measurements and numerical modelling. Eng Struct. 2014;80:435–443. doi: 10.1016/j.engstruct.2014.09.024
[32] Jain A, van Dalen K, Metrikine A, et al. Comparative analysis of the dynamic amplifications due to inhomogeneities at railway transition zones. In: Pombo J, editor. Proceedings of The Fifth International Conference on Railway Technology: Research, Development and Maintenance; (Civil-Comp Conferences; Vol. 1); United Kingdom: Civil-Comp Press; 2023.
[33] Wang H, Markine V, Liu X. Experimental analysis of railway track settlement in transition zones. Proc Inst Mech Eng F J Rail Rapid Transit. 2018;232(6):1774–1789. PMID: 30662168. doi: 10.1177/0954409717748789